10.21608/adjc.2024.243943.1419 Advanced Dental Journal
Volume 6 (2024) | Issue 4| Pages 656-665

Original Article

Effect of Variations of Field of View (Fov) and Milliampere (Ma) on Metal Artifacts in Cone Beam Computed Tomography:(In Vitro Study)

Roshan Adel[1], Noha Ossama Abdelaziz Issa [1], Walaa Samir Abdelfattah [2], Walaa Abd El Aty Ahmed[1]

[1] Oral Radiology Department, Faculty of Dentistry, Cairo University, Egypt

[2] Oral Radiology Department, Faculty of Dentistry, Beni Suef University, Egypt

Email: roshan.ahmed@dentistry.cu.edu.eg

Submitted: 4-11-2023
Accepted: 4-1-2024

Abstract

Aim: The aim of this study is to evaluate the effect of exposure parameters as milliampere (mA) and field of view (FOV) in CBCT on metal artifact of dental implant, Can change of milliampere (mA) and field of view (FOV) reduce the metallic artifacts in CBCT that result from metallic structures?

Subjects and methods: Four dry human mandibles with implants inserted in them, were scanned by using Planmeca ProMax® 3D Mid CBCT machine, using different values of FOV and mA, without the activation of MAR tool. Romexis® software was used for image analysis. For each implant linear measurements were measured (length & width), implants real length and width were used as gold standard.

Results: In general, the change of the size of FOV had no significant effect on metal artifacts reduction ($P > 0.05$), Also; it was the same on mA values, there was no significant effect on metal artifacts reduction ($P > 0.05$).

Conclusion According to the results of this study, Size of FOV and different values of mA of CBCT have no significant effect on the metal artifacts around dental implants.

Keywords: CBCT - Metal artifacts - Beam hardening artifact - Dental Implants – MAR – Metal artifacts reduction - metal artifact reduction protocols – mA – FOV.

I. INTRODUCTION

Over the past few decades, dentistry has made huge advancements, thanks to the shift to digital dentistry for diagnosis, treatment planning and surgical planning. Traditional radiologic examination methods, such as intraoral and panoramic radiographs, which are utilized for routine diagnosis in dentomaxillofacial area, are typically restricted to two dimensional views. To address the drawbacks of 2D imaging, such as anatomical overlap and distortions, three-dimensional imaging has become more necessary as the process of diagnosis and treatment planning has advanced in several dental sectors **(Gaêta-Araujo *et al.*, 2020)**.

Cone beam computed tomography (CBCT), which has gained widespread acceptance in

oral and maxillofacial surgery, is frequently available among dentists in the operating room. In comparison to traditional computed tomography (CT), CBCT offers the practitioner 3D and multiplanar views for precise diagnosis and treatment planning at a reasonable cost and with less radiation exposure **(Weiss and Read-Fuller, 2019)**.

The presence of artifacts in the CBCT images that prevent the proper visualization of the peri-implant bone that is essential for the success of implants has not been solved yet, in spite of the efforts performed to reduce them **(Demirturk Kocasarac et al. 2019)**.

An artifact is, by definition, any distortion or inaccuracy in the image that is not related to the object being radiographed. It is regarded as one of the primary reasons for image quality degradation, and in extreme situations, the artifact entirely ruins the image. All CT and cone beam CT scanners produce reconstructed images with artifacts due to the technical characteristics of the device, such as geometry, beam energy, and the back projection image generation process **(Demirturk Kocasarac et al. 2019).**

The beam hardening artifact is one of several forms of artifacts that have been described with CBCT and is frequently seen as dark streaks resulting from high attenuation objects **(Fox et al. 2018).** When an x-ray beam made up of polychromatic energies travels through an object, it is thought to produce common artifact of beam hardening, which causes selective attenuation of lower energy photons. That increases the mean beam energy since only photons with higher energies are left to contribute to the beam, conceptually similar to a high-pass filter (**Shokri et al., 2019)**. Beam hardening artifacts typically appear as two distinct artifacts on the final CBCT images: a cupping artifact and dark bands or streaks **(Shokri et al., 2019).**

The quality and characteristics of the CBCT images, which may include artifacts, contrast resolution, and noise, can be affected by several factors, including the X-ray beam quantity and quality, mA, rotation arc, field of view (FOV), and pixel size. One of the biggest things that lowers the quality of the image is thought to be metal related artifacts **(Panjnoush et al., 2016).**

Numerous software and imaging techniques have been created in an attempt to treat the issue of how artifacts affect the final CBCT image. Filtration, anti-scatter grids, calibration correction, and beam hardening correction software were all used by manufacturers to reduce beam hardening **(Jaju et al., 2013).**

One of the most crucial hardware components that must be carefully chosen in order to obtain more trustworthy reliable and accurate readings is the field of view **(Abdelkarim, 2019).** Additionally, one of the primary exposure parameters that works to lessen the appearance of CBCT artifacts is the milliampere (mA) **(Freitas et al. 2018).**

That's why this study was carried out to throw the light on the effect of variation of exposure parameters of FOV and mA on reduction of metal artifact resulting from metallic structures in CBCT scans.

II. SUBJECTS AND METHODS

The study was conducted using four human dry mandibles that were totally edentulous. The used models were facilitated from (faculty of medicine, Cairo University).

Human jaw mandibles were drilled to allow for titanium dental implants placement (from Root Company) of either single implants on left side or two adjacent double implants on right side randomly drilled in different positions on each jaw. Then each mandible was covered by two layers of dental pink wax for soft tissue stimulation (Figure 1).

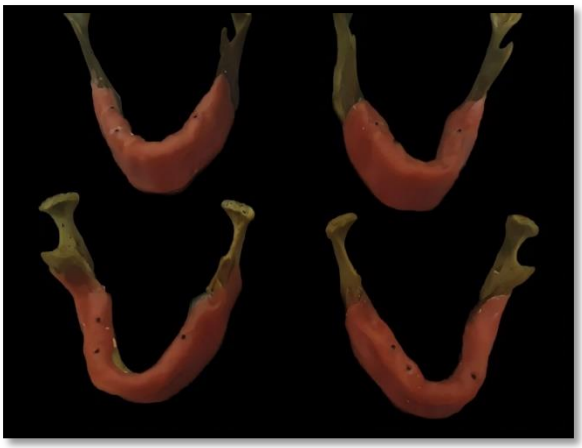

Figure (1): Four dry human mandibles that are totally edentulous with implant placement.

CBCT Imaging of Jaw Models

1. Standardization of the positioning of the mandible during scanning:

A compressed piece of cork was cut to support the mandible during scan. That piece of cork was marked by a marker for the placement each time of scan for standardization achievement. The same piece of cork was used for all scans (Figure 2).

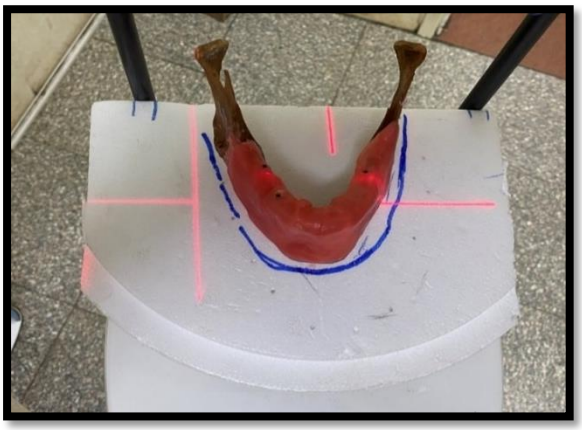

Figure (2): the compressed piece of cork with markers for standardization during scan.

2. Exposure Parameters:

Jaw models were scanned in the Oral and Maxillofacial Radiology Department, Faculty of Dentistry, Cairo University, using CBCT machine Planmeca ProMax® 3D Mid, by adjusting the following exposure parameters:

I1 (Index test): Cone beam CT imaging and real measurements of each dental implant used.

I2: CBCT with Field of view **XS** with its default milliampere **5.6 mA.**
I3: CBCT with Field of view **S** with its default milliampere **6.3 mA.**
I4: CBCT with Field of view **M** with its default milliampere **8 mA.**
I5: CBCT with Field of view **L** with its default milliampere **10 mA.**
I6: CBCT with Field of view **XL** with its default milliampere **12.5 mA.**

All these scans were taken using default exposure CBCT parameter; kVp was 90, with a voxel size of 0.4 mm. All the above exposure parameters were kept constant in all the scans.

3. Image Processing:

Primary reconstruction and processing of the scans as well as image analysis were done using Romexis® software (Planmeca-Helsinki-Finland). For each dry mandible, 5 CBCT scans with different FOV set ups (XS-S-M-L-XL) and mA (5.6-6.3-8-10-12.5) were acquired as previously mentioned. 5 scans with Jaw view, 5 scans with right teeth scan and 5 scans with left teeth scan (quadrant scan). Consequently, each jaw model had fifteen CBCT scans with different FOV, mA, views.

Image Analysis

Image analysis in the current study included quantitative assessment, that was done for implants linear measurements (length and width). On the axial image, the coronal plane was rotated to be perpendicular to the buccal cortical plate of bone adjacent to the implant under investigation. On the coronal and sagittal images, the orthogonal axes were adjusted to pass along the long axis of the implant. The image showing the maximum dimension of the implant in the coronal and sagittal directions was selected. The measurements of implant length and width were proceeded in bucco-lingual direction on coronal images (Figure 3).

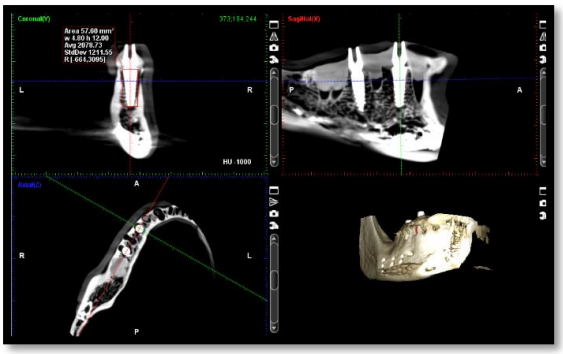

Figure (3): Orientation of orthogonal planes for measuring implant dimensions.

Implant length was measured by considering it as the perpendicular distance between two tangential lines to the base and apex of the implant in the bucco-lingual (coronal) (Figure 4).

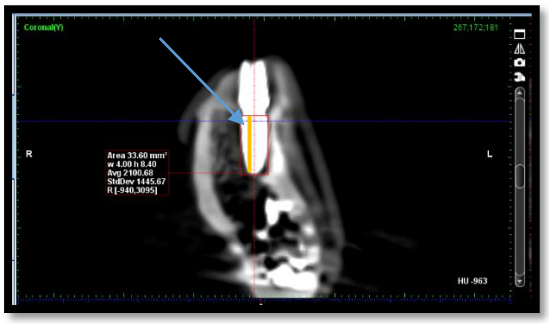

Figure (4): Measurements of implant length using rectangular measuring tool.

Implant width was measured by considering it as the perpendicular distance between two tangential lines to the implant base in the bucco-lingual (coronal) (Figure 5).

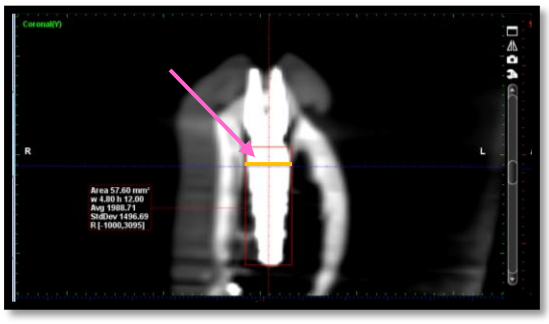

Figure (5): Measurements of implant width using rectangular measuring tool.

Blinding & Inter and Intra-Observer Agreement

The assessment was done by three oral radiologists with different experience in three separate sessions. The three observers were blind to the results of each other, but there were only two assessments that were used for statistical analysis and inter-observer agreement was evaluated.

Sample size calculation:

A power analysis was designed to have adequate power to apply a statistical test of the null hypothesis that there is no difference between tested groups. By adopting an alpha level of (0.05) a beta of (0.2) i.e., power=80% and an effect size (f) of (0.38) calculated based on the results of a previous study1; the predicted sample size (n) was a total of (80) cases of mandibular quadrant. Sample size calculation was performed using G*Power version 3.1.9.72

Statistical methods

Numerical data were presented as mean and standard deviation (SD) values. They were explored for normality by checking the data distribution and using Shapiro-Wilk test. Measurement data were normally distributed and were analyzed using paired t-test. Difference data were non-parametric and were analyzed using Freidman's test. Inter-rater reliability was analyzed using Intra-class correlation coefficient (ICC). The significance level was set at $p \leq 0.05$. Statistical analysis was performed with R statistical analysis software version 4.1.3 for Windows1.

III. RESULTS

1.Inter-observer reliability:

Inter-observer reliability was presented in table (1)

There was a strong agreement between both observers which was statistically significant (ICC=0.999, p<0.001).

Table (1): Inter-observer reliability

ICC	95% CI	p-value
0.999	0.999:0.999	**<0.001***

*; significant ($p \leq 0.05$) ns; non-significant (p>0.05)

2.Difference from actual readings:

Differences from actual readings were presented in table (2).

- **Width:**

For all groups, after scan measurement was significantly higher than real measurement (p<0.001).

- **Height:**

For (M-8), after scan measurement was significantly higher than real measurement (p=0.044). For other groups, the difference was not statistically significant (p>0.05).

3.Comparison of devices' accuracy:

Comparison of devices' accuracy was presented in table (3) and figure (35 & 36)

- **Width:**

There was no significant difference between the different groups (p=0.542). The highest value was found in (L-10) (0.95±0.47), followed by (M-8) (0.91±0.50), then (XL-12.5) (0.86±0.42), and (S-6.3) (0.82±0.48), while the lowest value was found in (XS-5.6) (0.80±0.42).

- **Height:**

There was no significant difference between values found in different groups (p=0.551). The highest value was found in (XS-5.6) (0.23±0.37), and (M-8) (0.23±0.54), followed by (XL-12.5) (0.22±0.58), and (L-10) (0.22±0.53), while the lowest value was found at (S-6.3) (0.21±0.51).

Table (2): Differences from actual readings

Measurement	Group	(mean±SD) mm		Mean difference	95% CI for mean difference		p-value
		Real measurement	Measurement after scan		Lower	Upper	
Width	**XS-5.6**	3.81±0.72	4.55±0.69	-0.74	-0.96	-0.52	**<0.001***
	S-6.3	3.81±0.72	4.62±0.75	-0.82	-1.02	-0.61	**<0.001***
	M-8	3.81±0.72	4.72±0.81	-0.91	-1.12	-0.7	**<0.001***
	L-10	3.81±0.72	4.73±0.71	-0.92	-1.15	-0.7	**<0.001***
	XL-12.5	3.81±0.72	4.67±0.79	-0.86	-1.04	-0.68	**<0.001***
Height	**XS-5.6**	10.50±2.38	10.67±2.43	-0.17	-0.34	0.01	**0.057ns**
	S-6.3	10.50±2.38	10.71±2.26	-0.21	-0.42	0.01	**0.058ns**
	M-8	10.50±2.38	10.73±2.22	-0.23	-0.46	-0.01	**0.044***
	L-10	10.50±2.38	10.72±2.21	-0.22	-0.44	0.01	**0.059ns**
	XL-12.5	10.50±2.38	10.72±2.22	-0.22	-0.46	0.03	**0.079ns**

*; significant ($p \leq 0.05$) ns; non-significant (p>0.05)

Table (3): Comparison of devices' accuracy

Measurement	Difference from real measurement (mm) (mean±SD)					p-value
	XS-5.6	S-6.3	M-8	L-10	XL-12.5	
Width	0.80 ± 0.42^{A}	0.82 ± 0.48^{A}	0.91 ± 0.50^{A}	0.95 ± 0.47^{A}	0.86 ± 0.42^{A}	**0.542ns**
Height	0.23 ± 0.37^{A}	0.21 ± 0.51^{A}	0.23 ± 0.54^{A}	0.22 ± 0.53^{A}	0.22 ± 0.58^{A}	**0.551ns**

Values with different superscript letters within the same horizontal row are significantly different *; significant ($p \leq 0.05$) ns; non-significant (p>0.05).

IV. DISCUSSION

Since CBCT was introduced for the maxillofacial region in 1998, it has become an important and established diagnostic tool for the clinical assessment and treatment planning of patients seeking dental implants **(Hatcher, Dial and Mayorga, 2003)**. One of the main advantages of the CBCT modality over that of medical conventional CT is the reduction in the actual size which is approximately one quarter to one fifth of that of CT, which consequently affects the overall cost of both machines. This advantage may be of great concern to radiologists or dentists, but when considering the patient as an important factor, the reduction in the overall radiation dose and scanning time can be considered to favor CBCT imaging over CT **(Scarfe and Farman, 2008)**.

Another advantage of CBCT; is that it provides images of highly detailed structures, by producing images with submillimeteric isotropic voxels, that range from 0.4 mm to as low as 0.076 mm, allowing for secondary reconstruction of the obtained images in the 3 different orthogonal planes; axial, coronal, and sagittal, as well as 3D reconstruction of the patient's data. All of these factors render CBCT the best choice for implant site assessment for patients seeking dental implants **(Scarfe and Farman, 2008),** in addition to providing good assessment of the anatomical and vital structures near the proposed implant sites **(Amin *et al.,* 2013)**.

All the previously mentioned reasons empower the choice that CBCT should be used in preoperative implant planning and positioning., but when coming to implants post-insertion assessment cases, CBCT is recommended to be used as the imaging modality in cases of potential implant failure, mobility or paresthesia, according to the recent guidelines " **(Jacobs *et al.,* 2018)**. Such usage may lead the radiologists to face some challenges, mainly the inherent CBCT artifacts, which include any distortion or error in the image that is unrelated to the subject being studied **(Scarfe and Farman 2008) & (Schulze *et al.,* 2011)**.

The main concern in the current study was to evaluate the effect of these resulting artifacts, and assuming the best available technique to reduce their effect on the overall final CBCT images, while exposing the patient to the least acceptable, optimum radiation dose according to the ALARA principle: "As Low As Reasonably Achievable" **Jaju and Jaju, (2015),** or more recently, the ALADA principle "As Low As Diagnostically Achievable" **(Jacobs *et al.,* 2018).**

(Safi, Ahsaie and Amiri, 2022) used 2 different FOV to assess their effect on CBCT artifacts caused by metal artifacts from titanium Implants on exomass (zone outside the FOV) and the result showed that there was increase on exomass size by using smaller FOV and image quality not affected by that.

Another study by **(Shokri *et al.,* 2022)**, also used two different FOV to detect the amount of artifacts around the titanium implants and found that increasing in FOV could reduce artifacts and that was not in accordance with our study, probably due to using bovine rib bone blocks in his study whereas our study used dry human mandibles.

Kvp exposure parameter was maintained constant during scanning to avoid its effect. Even though other studies investigated the combined effects of both mA & kVp **(Panjnoush *et al.,* 2016), (L Bohner, Tortamano and Marotti, 2017) & (Pinto *et al.,* 2017)** and the effect of the mA alone **(Sur *et al.,* 2010).** But in our study, we believe that studying the effect of FOV and mA, would be more effective as supported by **(Shokri *et al.,* 2019) and (Mehdizadeh, Erfani and Soltani, 2022).**

Each human mandible was scanned with 5 different FOV values, different mA values and different implants distribution, to ensure different implants positions and configurations, all over the mandible (anterior or posterior, single or double).

The accuracy of the linear measurements and the measurement tool (Romexis® software), were one of our main concerns during this study, the used software was found to be accurate in many studies concerning the linear measurements of the implants, giving statistically insignificant difference from that of the gold standard real implants measurements, as in the study done by **(Khongkhunthian, Jomjunyong and Reichart, 2017).**

The qualitative assessment is not concerned with the numerical representativeness of the outcome of the study, but with a deeper understanding of the subject in a more subjective way, relying on the visual detectability and preference of the observer. On the other side, in the quantitative assessment, the data to be analyzed can be quantified into numbers, by using more standardized instruments and a mathematical language **(Freitas *et al.*, 2018).**

Quantitative assessment of the accuracy of measurements of implants dimensions (Implants length & width) was previously done by **(Patcas *et al.*, 2012), (Vazquez, 2016) & (Silveira-Neto *et al.*, 2017).** In their studies, they compared mainly the implant length before and after with different exposure parameters.

In our study, there was a very strong inter-observer reliability for linear measurements of implants length & width for both single and double implants. A study by **(Amin *et al.*, 2013)** was done to study the validity of cone beam dental image for measuring the implants linear measurements and its limitations in terms of distortion, by using clinically placed implant on patients. They reported the same strong agreement for implants length and width measurements accuracy, that were measured by using the same software Planmeca Romexis used in our study, when the readings were repeated by the same observer or between the observers.

Considering the accuracy of implants linear measurements width and height, for width all groups after scan measurement was significantly higher than real measurement ($p<0.001$) and for height group of FOV (M) and mA (8) after scan measurement was significantly higher than real measurement ($p=0.044$). For other groups, the difference was not statistically significant ($p>0.05$).

In the study carried out by **(Shokri *et al.*, 2019)** to evaluate the effect of mA and FOV of CBCT on a metal artifact of dental implants placed in different bone densities showed that the amount of artifact was lower in small FOV than the large one ($P < 0.05$) and the change of mA had no effect on metal artifacts ($P > 0.05$), That result about FOV doesn't agree with our study and that may be due to using different imaging system and measurement technique.

Another study done by **(Elshenawy *et al.*, 2019)** to evaluate the effect of different FOV values on dimensional accuracy of CBCT scanning found that both large and medium FOV values showed a statistically significant difference, which might be translated into clinical relevance only in thickness measurements and increasing the FOV size together with voxel size could affect the accuracy of CBCT linear measurements adversely, especially during evaluating small distances.

However, this study had some limitations- which were mentioned by the authors themselves- which yielded their results unreliable. The first limitation was that they used only one implant in the model for each scan, also, they did not incorporate other artifacts forming structures to the models. They claimed their choice to the reason that they did not want to increase the intensity of the artifacts in the final images.

A study done by **(Mehdizadeh, Erfani and Soltani, 2022)** to assess the effectiveness of the FOV on linear measurements of CBCT scans showed that the measurements of the small and large FOV values had excellent correlation coefficient when compared with those obtained with dry skull, as the linear

measurements that were obtained by CBCT images in large and small FOV values were not significantly different from those on dry skulls.

Limited number of studies have been published about the quantitative assessment of the artifacts, and mostly were around dental implants, except for **(Omar, Abdelsalam and Hamed, 2016)** In their study, they quantitatively assessed metallic artifacts of different restorative materials in terms of volume not length, using two different segmentation methods by Simplant software & **(Sheridan et al., 2018)** who quantitively assessed the areas of the artifacts surrounding 20 porcelain fused to metal crowns scanned with different FOV sizes.

Another study by **(Machado *et al.*, 2018)**, quantitatively assessed the effect of the artifacts surrounding the dental implants by using grey values, where they concluded the effect of the anatomical position of the implants which were distributed to be isolated or close to other implants, by result of that the maxillary implants had fewer artifacts and the posterior region produced less artefacts than the anterior one. Finally, the study concluded that the metal artifacts in CBCT images are always produced by dental implants, and these artifacts are affected by the anatomical placement in the dental arch.

The results of the above mentioned study was not in accordance with the results of our study, this may be due to the following reasons: firstly, the methodology of this study was different from ours, as we did not evaluate the grey values in vicinity of the implants, but we depended on linear measurements for the evaluation of the effect of exposure parameters of FOV and mA on the reduction of the artifacts effects of the surrounding structures to the metallic objects. Secondly, they used a different CBCT machine than the one we used in our study. Consequently, our quantitative analysis and the type of machine used in our study yielded much more accurate results.

No approaches nor algorithms were employed in this study to reduce artifacts in CBCT images. It is proposed that their effectiveness be examined in future studies in order to eliminate CBCT image artifacts. In our research, we used human jaw mandibles for better clinical simulation and scanned them on the same machine, with the same software performing analysis and measurements, but for more accurate findings, various CBCT equipments and variable software could be employed.

Our findings demonstrated that artifacts are always present near dental implants. As a result, doctors must use caution when interpreting these images. Unlike many clinicians' beliefs that altering the amperage can affect the amount of artifacts, our findings revealed that changing the exposure parameters of mA and FOV of CBCT has no effect on the decrease of metal artifacts.

V. CONCLUSION:

From the present work, and within its limitations, the following conclusions could be reached:

1- Changing FOV has no significant effect on reduction of the effect of the metal induced artifacts related to dental implants.

2- Changing mA has no significant effect on reduction of the effect of the metal induced artifacts related to dental implants.

Conflict of Interest:

The authors declare no conflict of interest.

Funding:

This research received no specific grant from any funding agency in the public, commercial, or not-for-profit sectors.

Ethics:

This study protocol was approved by the ethical committee of the faculty of dentistry-Cairo university on: 26/10/2021, approval number: 91021

VI. REFERENCES

1. Abdelkarim, A. (2019) 'Cone-beam computed tomography in orthodontics', *Dentistry Journal*. Available at: https://doi.org/10.3390/dj7030089.
2. Amin, L.I.B.M. *et al.* (2013) 'Validity of cone beam computed tomography (CBCT) on estimation of implant fixture length', *International Medical Journal*, 20(3), pp. 355–358.
3. Demirturk Kocasarac, H. *et al.* (2019) 'Evaluation of artifacts generated by titanium, zirconium, and titanium–zirconium alloy dental implants on MRI, CT, and CBCT images: A phantom study', *Oral Surgery, Oral Medicine, Oral Pathology and Oral Radiology*, 127(6), pp. 535–544. Available at: https://doi.org/10.1016/j.oooo.2019.01.074.
4. Elshenawy, H. *et al.* (2019) 'Influence of small, midi, medium and large fields of view on accuracy of linear measurements in CBCT imaging: Diagnostic accuracy study', *Open Access Macedonian Journal of Medical Sciences*, 7(6), pp. 1037–1041. Available at:https://doi.org/10.3889/oamjms.2019.232.
5. Fox, A. *et al.* (2018) 'A Novel Method for Characterizing Beam Hardening Artifacts in Cone-beam Computed Tomographic Images', *Journal of Endodontics*, 44(5), pp. 869–874. Available at: https://doi.org/10.1016/j.joen.2018.02.005.
6. Freitas, D.Q. *et al.* (2018) 'Influence of acquisition parameters on the magnitude of cone beam computed tomography artifacts', *Dentomaxillofacial Radiology*, 47(8). Available at: https://doi.org/10.1259/dmfr.20180151.
7. Gaêta-Araujo, H. *et al.* (2020) 'cone beam computed tomography in dentomaxillofacial radiology: A two-decade overview', *Dentomaxillofacial Radiology*, 49(8), pp. 1–20. Available at:https://doi.org/10.1259/DMFR.20200145.
8. Hatcher, D.C., Dial, C. and Mayorga, C. (2003) 'Cone beam CT for pre-surgical assessment of implant sites.', *Journal of the California Dental Association*, 31(11), pp. 825–833. Available at: https://doi.org/10.1080/19424396.2003.12224265.
9. Jacobs, R. *et al.* (2018) 'Cone beam computed tomography in implant dentistry: Recommendations for clinical use', *BMC Oral Health*, 18(1), pp. 1–16. Available at: https://doi.org/10.1186/s12903-018-0523-5.
10. Jaju, P.P. *et al.* (2013) 'Artefacts in cone beam CT', *Open Journal of Stomatology*, 03(05), pp. 292–297. Available at: https://doi.org/10.4236/ojst.2013.35049.
11. Jaju, P.P. and Jaju, S.P. (2015) 'Isd-45-263', *Cone-beam computed tomography: Time to move from ALARA to ALADA*, pp. 263–265.
12. Khongkhunthian, P., Jomjunyong, K. and Reichart, P.A. (2017) 'Accuracy of cone beam computed tomography for dental implant treatment planning', *Chiang Mai University Journal of Natural Sciences*, 16(1), pp. 51–62. Available at: https://doi.org/10.12982/cmujns.2017.0005.
13. L Bohner, L.O., Tortamano, P. and Marotti, J. (2017) 'Accuracy of linear measurements around dental implants by means of cone beam computed tomography with different exposure parameters', *Defile:///D:/Master/Papers/Exposure parameters/2016-Influence of exposure parameters on the detection of simulated root fractures in the.pdfntomaxillofacial Radiology*, 46(5). Available at: https://doi.org/10.1259/dmfr.20160377.
14. Machado, A.H. *et al.* (2018) 'Effect of anatomical region on the formation of metal artefacts produced by dental implants in cone beam computed tomographic images', *Dentomaxillofacial Radiology*, 47(3). Available at: https://doi.org/10.1259/dmfr.20170281.
15. Mehdizadeh, M., Erfani, A. and Soltani, P. (2022) 'Comparison of the accuracy of linear measurements in CBCT images with different field of views', *Clinical and Laboratorial Research in Dentistry*, 2022, pp. 1–4. Available at: https://www.revistas.usp.br/clrd/article/view/194059.
16. Omar, G., Abdelsalam, Z. and Hamed, W. (2016) 'Quantitative analysis of metallic artifacts caused by dental metallic restorations: Comparison between four CBCT scanners', *Future Dental Journal*, 2(1), pp. 15–21. Available at: https://doi.org/10.1016/j.fdj.2016.04.001.

17. Panjnoush, M. *et al.* (2016) 'Effect of Exposure Parameters on Metal Artifacts in Cone Beam Computed Tomography.', *Journal of dentistry (Tehran, Iran)*, 13(3), pp. 143–150. Available at: http://www.ncbi.nlm.nih.gov/pubmed/28392810%0Ahttp://www.pubmedcentral.nih.gov/articlerender.fcgi?artid=PMC5376540.
18. Patcas, R. *et al.* (2012) 'Accuracy of linear intraoral measurements using cone beam CT and multidetector CT: A tale of two CTs', *Dentomaxillofacial Radiology*, 41(8), pp. 637–644. Available at: https://doi.org/10.1259/dmfr/21152480.
19. Pinto, M.G.O. *et al.* (2017) 'Influence of exposure parameters on the detection of simulated root fractures in the presence of various intracanal materials', *International Endodontic Journal*, 50(6), pp. 586–594. Available at: https://doi.org/10.1111/iej.12655.
20. Safi, Y., Ahsaie, M.G. and Amiri, M.J. (2022) 'Effect of the Field of View Size on CBCT Artifacts Caused by the Presence of Metal Objects in the Exomass', *International Journal of Dentistry*, 2022. Available at: https://doi.org/10.1155/2022/2071108.
21. Scarfe, W.C. and Farman, A.G. (2008) 'What is Cone-Beam CT and How Does it Work?', *Dental Clinics of North America*, 52(4), pp. 707–730. Available at: https://doi.org/10.1016/j.cden.2008.05.005.
22. Schulze, R. *et al.* (2011) 'Artefacts in CBCT: A review', *Dentomaxillofacial Radiology*, 40(5), pp. 265–273. Available at: https://doi.org/10.1259/dmfr/30642039.
23. Sheridan, R.A. *et al.* (2018) 'The effect of implant-induced artifacts on interpreting adjacent bone structures on cone-beam computed tomography scans', *Implant Dentistry*, 27(1), pp. 10–14. Available at: https://doi.org/10.1097/ID.0000000000000684.
24. Shokri, A. *et al.* (2019) 'Effect of exposure parameters of cone beam computed tomography on metal artifact reduction around the dental implants in various bone densities', *BMC Medical Imaging*, 19(1), pp. 1–10. Available at: https://doi.org/10.1186/s12880-019-0334-4.
25. Shokri, A. *et al.* (2022) 'Comparison of the amount of artifacts induced by zirconium and titanium implants in cone-beam computed tomography images', *BMC Medical Imaging*, 22(1), pp. 1–10. Available at: https://doi.org/10.1186/s12880-022-00884-5.
26. Silveira-Neto, N. *et al.* (2017) 'Peri-implant assessment via cone beam computed tomography and digital periapical radiography: An ex vivo study', *Clinics*, 72(11), pp. 708–713. Available at: https://doi.org/10.6061/clinics/2017(11)10.
27. Sur, J. *et al.* (2010) 'Effects of tube current on cone-beam computerized tomography image quality for presurgical implant planning in vitro', *Oral Surgery, Oral Medicine, Oral Pathology, Oral Radiology and Endodontology*, 110(3), pp. e29–e33. Available at: https://doi.org/10.1016/j.tripleo.2010.03.041.
28. Vazquez, L. (2016) 'Influence of image-viewers and artifacts on implant length measurements in cone-beam computed tomography: an in vitro study.' Available at: https://onlinelibrary.wiley.com/doi/full/10.1002/cre2.18.
29. Weiss, R. and Read-Fuller, A. (2019) 'Cone Beam Computed Tomography in oral and maxillofacial surgery: An evidence-based review', *Dentistry Journal*, 7(2), pp. 1–23. Available at: https://doi.org/10.3390/dj7020052.